SLAC-PUB-9391
August 2002

# Power density spectral analysis as a method of compact object determination in X-ray binary systems

John Lee
DOE Energy Research Undergraduate Laboratory Fellowship Program
Taylor University
Stanford Linear Accelerator Center
Menlo Park, CA

August 14, 2002

Prepared in partial fulfillment of the requirements of the DOE ERULF Program under the direction of Pablo Saz Parkinson and Kaice Reilly in Experimental Group K at SLAC

**Work supported by the Department of Energy contract** DE-AC03-76SF00515.

# Contents



# List of Figures



# List of Tables

# 1 Abstract

Power density spectral analysis as a method of compact object determination in X-ray binary systems. J. Lee (Taylor University, Upland, IN, 46989), P. Saz Parkinson & K. Reilly (Stanford Linear Accelerator Center, Menlo Park, CA 94025).

Mass determinations and X-ray energy spectral analyses are among the methods used to distinguish between the types of compact objects present in X-ray binary systems. We test a method of distinguishing between neutron stars and black holes proposed by Sunyaev and Revnivtsev where power density spectra are used, particularly in the 500-1000Hz range. Sunyaev and Revnivtsev found that only neutron stars appear to have significant power in this frequency range. We apply this criterion to 12 X-ray binary systems (six neutron stars and six black holes) using USA data and cannot reproduce Sunyaev and Revnivtsev's result. The reason for this discrepancy is most likely a USA instrumental effect which manifests itself as excess power in the frequency range of interest. Future work on correcting this probelm should provide more accurate analyses that may yield a different result.

–

## 2 Introduction

Galactic X-ray binary systems can contain different kinds of compact objects: white dwarfs, neutron stars, and black holes (Shabad 2000). When studying a particular X-ray source, it is important to be able to determine which kind of compact object is present. White dwarf systems are relatively easy to distinguish because of their low X-ray luminosity and much larger surface area, which lend themselves to easier optical identification (Shabad 2000; Tanaka and Lewin 1995). There are several methods that are commonly used to distinguish between neutron stars (NSs) and black hole candidates (BHCs). The most common is the use of optical observations to constrain the mass of the system. Also, Type I X-ray bursts or steady pulsations are features unique to neutron stars and would not be present in black holes. However, when these types of X-ray phenomena are not detected and when accurate mass determinations cannot be made, it is necessary to use different techniques. One of these techniques is the study of the emmitted energy spectrum of the system. A very soft spectrum or a hard energy tail are generally signs that the object is a BH, though this is not always the case. (Tananbaum et al. 1972; Suniaev and Truemper 1979; Tanaka and Shibazaki 1996).

Sunyaev and Revnivtsev (SR, 2000) proposed a new method which uses the power density spectrum (PDS) in the frequency range of 500-1000 Hz to determine what type of compact object is present. Using data from the Rossi X-ray Timing Explorer (RXTE) experiment, SR found that only neutron stars seem to have significant power up to several hundred Hz. Based on these results, they concluded that if a source does not have a strong decline in its PDS up to several hundred Hz, it should be classified as a NS. However, it is important to note that an object may be a neutron star and not have significant power in this range. Hence, the absence of power up to several hundred Hz does not indicate the presence of a black hole. SR maintained that the power in the 500-1000 Hz range in NSs was due to phenomena occuring at the boundary layer between the NS surface and accretion disk. Because a black hole does not have a surface, these effects would not be expected.

In the present work, SR's method is applied to six BHCs and six NSs in order to determine if there is indeed a difference in their high frequency PDS, and if this type of distinction can be made using the Unconventional Stellar Aspect (USA) instrument.

USA was one of nine instruments that flew onboard the *Advanced Research and Global Observation Satellite* (ARGOS). The observations used for this work took place during the years 1999-2000 (see Table 1 for details). The data from each source was first run through a series of cuts that eliminated data with high background. Next, PDS were created using a Fast Fourier Transform (FFT) routine. Finally, the PDS for each BHC was scaled based on its mass and comparisons were then made between NS and BHC spectra.

## 3 Methods

The data from each source studied in this paper is the compilation of many different observations. This is due to the polar orbit of ARGOS, which limited individual USA observations to 10-15 minutes. USA had five modes of observation (for details, see Shabad 2000). We used only observations in USA modes 1 and 2, with 32 $\mu$s timing resolution and 16 channels of energy resolution. For the most part, we used channels 1-14 and excluded channels 0 and 15. Generally, channels 1-14 provide the most accurate data, although in one case (Cyg X-1), channels 0 and 15 were included to alleviate an instrumental effect. Furthermore, only observations with at least 100 cts $s^{-1}$ were used. After these preliminary cuts, the data was run through more specific cuts intended to eliminate observation spans with high background.

| *Source* | *Type* | *Amt of Data* | *Mass* | *Observation Dates* |
|---|---|---|---|---|
| Aql X-1 | NS | 54ks | $1.4M_\odot$ | Y1999_D147-Y2000_D295 |
| Crab | NS | 58ks | $1.4M_\odot$ | Y1999_D314-Y2000_D319 |
| Cyg X-2 | NS | 121ks | $1.4M_\odot$ | Y1999_D194-Y2000_D289 |
| EXO 0748 | NS | 78ks | $1.4M_\odot$ | Y2000_D009-Y2000_D144 |
| GX 349 | NS | 40ks | $1.4M_\odot$ | Y1999_D256-Y2000_D230 |
| GX 354 | NS | 75ks | $1.4M_\odot$ | Y1999_D228-Y2000_D280 |
| Cyg X-1 | BHC | 414ks | $10.1M_\odot$ | Y1999_D163-Y1999_D365 |
| GRS 1915 | BHC | 141ks | $14M_\odot$ | Y1999_D179-Y2000_D320 |
| X 1630 | BHC | 44ks | $10M_\odot$ | Y1999_D164-Y1999_D228 |
| XTE 1118 | BHC | 100ks | $10M_\odot$ | Y2000_D102-Y2000_D215 |
| XTE 1550 | BHC | 49ks | $10.6M_\odot$ | Y2000_D105-Y2000_D170 |
| XTE 1859 | BHC | 91ks | $10M_\odot$ | Y1999_D288-Y1999_D348 |

Table 1: Source information. Mass values indicated were those used for scaling.

The USA detector has a coincidence veto mechanism to detect false counts. These false counts can be caused by electrons or other high energy particles that might strike the detector. When a hit is recorded in more than one wire, it is vetoed and not registered as a valid photon event. This system is about 99% effective. The veto rate, as well as other calculated quantities, can be used to indicate regions where high background is likely and these data are then eliminated. Other quantities that were used to eliminate potentially corrupted data were the offset angle between detector and source, the angle between the detector and the earth's limb, and the fraction of the average count rate to the calculated background. The parameters that were used to make the background cuts were not initially well known. Many adjustments were made before a satisfactory set of values was found that eliminated high background regions but still allowed for a significant enough body of data to be analyzed. Table 1 shows all the data we used for the different sources. The amount of data indicated is what was left after all the cuts were applied.

Once the troublesome data had been eliminated, it was possible to run FFTs on each source. The FFT algorithm divided up each observation into a length between .2 and 2 seconds, depending on the ideal length for the FFT. The time bin for the light curve was 96 $\mu$s and each FFT was root mean squared normalized and corrected by an appropriate deadtime model (Shabad 2000). The FFTs were geometrically binned with a minimum bin of 67Hz and a bin increase of 200%. These values were chosen because they provided the most accurate and easy to read FFTs. For each source, an FFT was performed which had five frequency bins. We have chosen these five, large bins because they provide a good way to find an average power over a spread of frequencies. This is very useful because we can then use these average power values to determine if there is indeed a difference in the 500-1000 Hz range between NSs and BHCs.

Before accurate comparisons could be made between the NS and BHC power spectra, the sources must be scaled according to their individual masses. For a compact object, it is generally accepted that characteristic frequencies scale inversely proportionally to the object's mass (Sunyaev and Revnivtsev 2000). Therefore, when dealing with comparatively heavy objects like black holes, this effect must be taken into account. It is well known that neutron star masses all fall around 1.4$M_\odot$ (Charles 1998). Thus, for our purposes, we assume that all the neutron stars have this mass and we scale only the black holes. This is done by dividing a black hole's mass by 1.4$M_\odot$ which provides the scale factor. Then, when performing the FFT, the minimum frequency, maximum frequency, and minimum width are all divided by this factor. After the FFT is completed, the frequency data is multiplied through by this factor while keeping the power the same. This effectively shifts the FFT to higher frequency per the appropriate scale factor. Three of the BHCs studied had relatively well known mass approximations and these were used. GRS 1915, XTE 1550, and Cyg X-1 have approximate masses of 14$M_\odot$, 10.56$M_\odot$, 10.1$M_\odot$, respectively (Vilhu 2002; Orosz et al. 2002; Herrero et al. 1995). For XTE 1859, X 1630, and XTE 1118, a rough estimate of 10$M_\odot$ was used (Uemura and The Vsnet Collaboration Team 2002; Markwardt et al. 2001). After the mass scaling was complete, it was possible to get an accurate comparison of the NSs and BHCs.

## 4 Results

To get a rough idea of what each source's power spectrum looked like, a higher frequency binned FFT was done for each source (Figs 1 & 2). It is on these plots that the first sign of the previously mentioned instrumental effect is noticeable.

The USA detector has what is believed to be a pile-up problem which, in timing analyses, manifests itself as excess power in the 400Hz range. This can be seen most obviously in the Cyg X-1 spectrum in Figure 1. This effect varies in intensity from source to source and this variability is based partly on each source's energy spectra. This effect poses a significant problem because it occurs very near the frequency range in which we are interested. Also, the problem is compounded when the BHCs are mass scaled. When the power spectra are shifted to higher frequency, this extra 400Hz power is shifted right into the kHz range which is the range in which BHCs should have very limited power. The mass scaling is necessary in order to get an accurate

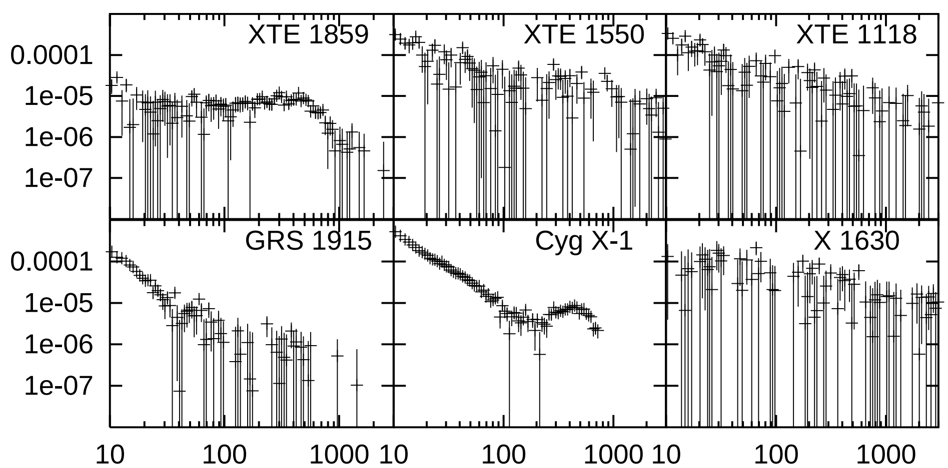


Figure 1: Power spectra of unscaled BHCs. Notice the intensity of power at 400 Hz in Cyg X-1.

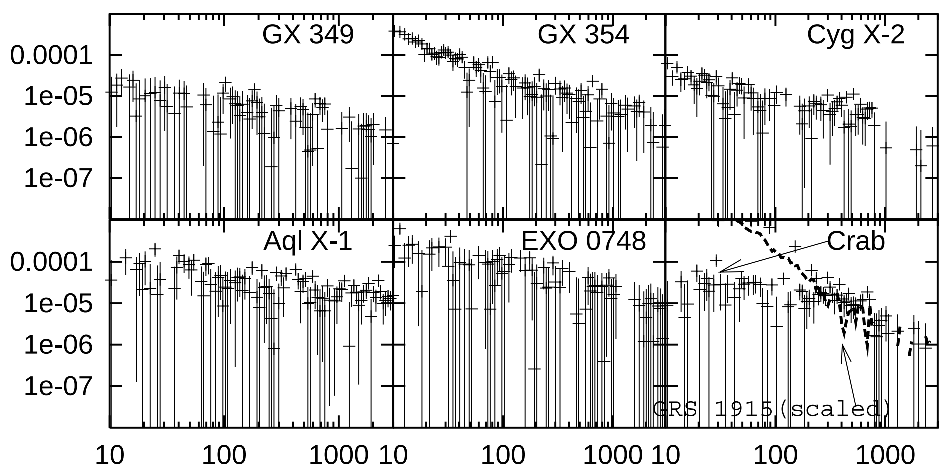


Figure 2: Power spectra of NSs.

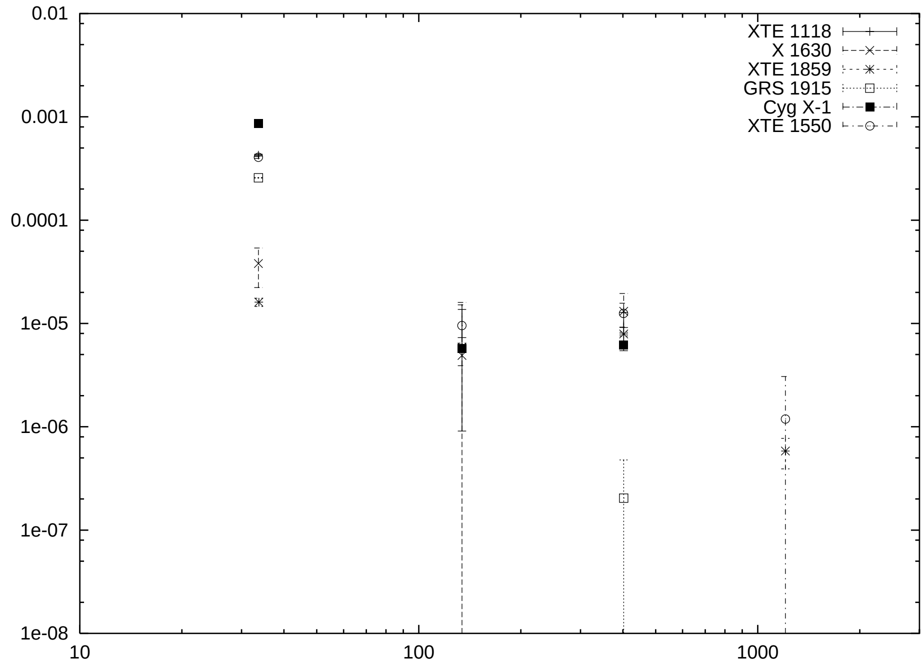


Figure 3: Large binned, unscaled BHC power spectra.

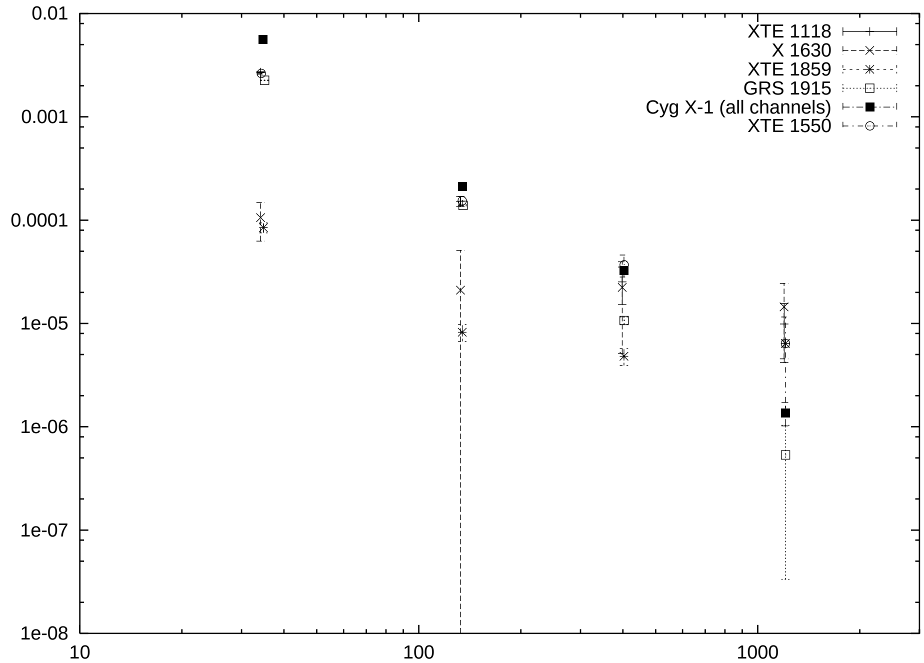


Figure 4: Large binned, scaled BHC power spectra.

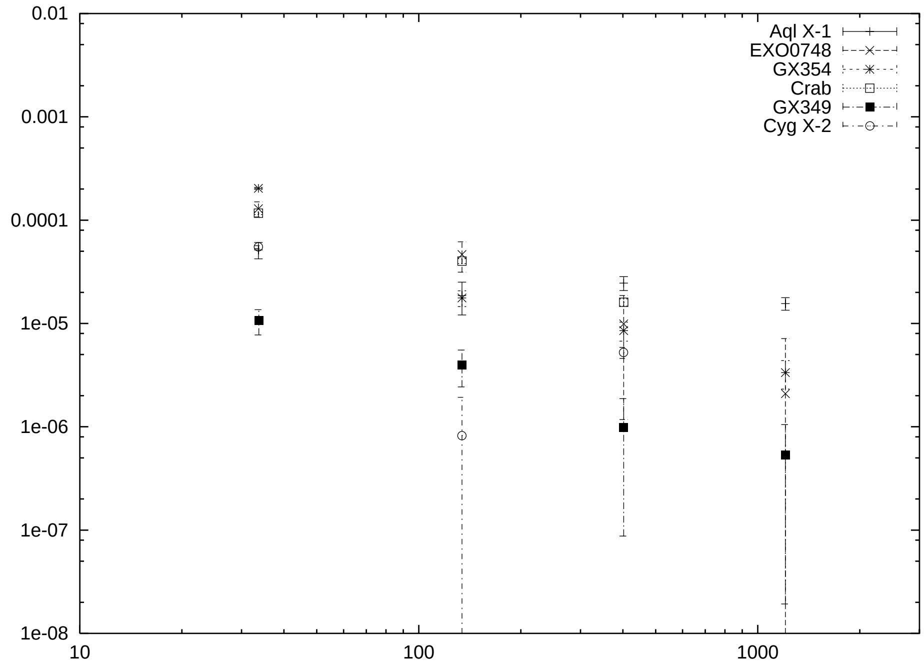


Figure 5: Large binned, NS power spectra.

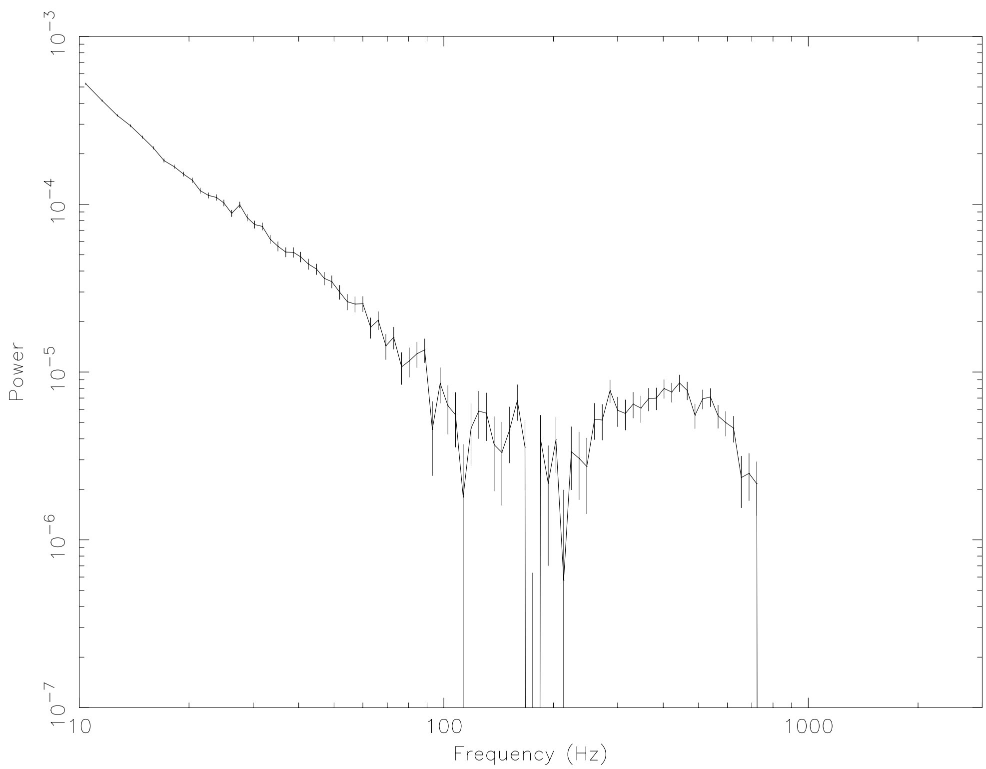


Figure 6: BHC Cyg X-1, with channels 1-14.

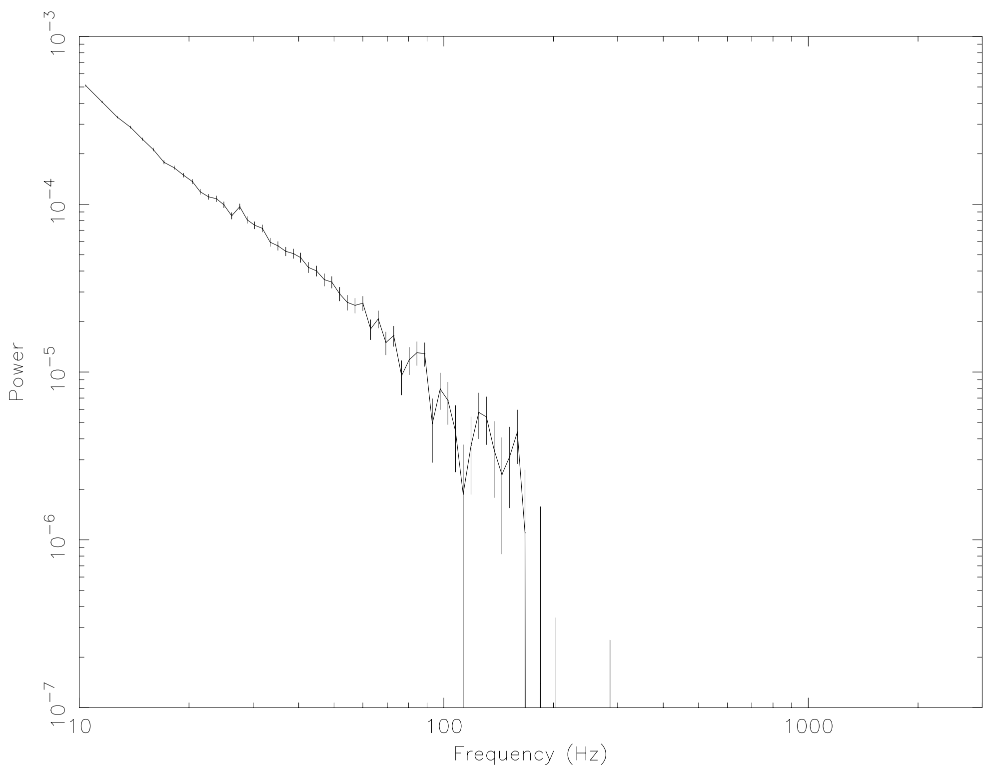


Figure 7: BHC Cyg X-1, with channels 0-15.

| *Frequency Range* | *NS Mean Power* | *BHC Mean Power* |
|---|---|---|
| 67-200 Hz | 2.1e-5 ±1.9e-5 | 1.1e-4 ±8.1e-5 |
| 200-600 Hz | 1.1e-5 ±8.4e-6 | 2.2e-5 ±1.2e-5 |
| 600-1800 Hz | 3.6e-6 ±6.0e-6 | 6.5e-6 ±5.2e-6 |

Table 2: Mean NS and BHC power in frequency ranges of interest.

comparison, but because of the instrumental effect, the scaling itself adds power to the region of greatest interest. Figure 3 shows the BHC power spectra before the scaling is done. As can be seen in comparison with Figure 5, the BHCs do seem to have significantly less power in the last three bins than the NSs. However, Figure 4 shows the scaled BHCs power spectra, and it can be seen that, in general, the power is higher than the NSs in the last three bins. Thus, in the 500-1000Hz region where SR saw decreased power in BHCs, we find the very opposite. The mean was calculated for all the NSs in each of the last three bins, and the same was done for the BHCs. For each bin, the BHC mean had higher power (see Table 2). Figure 2 shows the Crab NS compared with the mass scaled GRS 1915 BHC. As can be seen, there does not seem to be a significant difference in the frequency decline. A similar plot done by SR indiciated a significant difference even after scaling.

## 5 Discussion and Conclusions

Due to the high power in the 500-1000Hz range in almost every BHC, we must conclude that our results are in disagreement with SR. However, we are confident that this disagreement is almost completely due to a USA instrumental effect which is not yet fully understood. This is supported by the fact that the unscaled BHC power spectra do indeed appear to have less power in the frequency range of interest. Thus, most of the excess power comes from scaling, which ultimately comes from the 400Hz effect. In order to make a more accurate check of SR's result, we must first correct this 400Hz effect. This can be done by fitting many different sources in order to find a function that best represents this effect. This can then be subtracted off of a power spectrum, leaving an accurate remnant behind. Another solution that works on occasion is the inclusion of channels 0 and 15 in the FFT. This helps to minimize the excess power in the 400Hz range. Figure 6 shows the power spectrum of Cyg X-1 with channels 1-14. Figure 7 shows the same spectrum but with channels 0-15. As can be seen, this significantly reduces the effect. This is due to the fact that the inclusion of all the energy channels effectively cancels out the pile-up which adds the 400Hz signal. The range of energy channels that provides this canceling changes from source to source. Thus, another way to correct for the 400Hz effect is to find the specific energy channel range for each source that will best cancel it. Once work has been done to minimize or correct the instrumental effect, the analyses done in this paper could be done again, with perhaps a positive result.

## 6 Acknowledgements

I thank my mentors, Pablo Saz Parkinson and Kaice Reilly for their time, experience, and helpful discussion. I also thank the SLAC ERULF program directors, Sekazi Mtingwa and Helen Quinn, for their attention and thoughtful preparation. Finally, I thank SLAC and the U.S. Department of Energy for providing this fellowship.

## References

Charles, P. (1998). Black holes in our galaxy: observations. In *Theory of Black Hole Accretion Disks*. Cambridge University Press.

Herrero, A., R. P. Kudritzki, R. Gabler, J. M. Vilchez, and A. Gabler (1995, May). Fundamental parameters of galactic luminous OB stars. II. A spectroscopic analysis of HDE 226868 and the mass of Cygnus X-1. *AAP 297*, 556.

Markwardt, C., W. Focke, and J. Swank (2001). High Frequency Oscillations from the Black Hole Candidate XTE J1859+226. In *X-ray Emission from Accretion onto Black Holes*.

Orosz, J. A., P. J. Groot, M. van der Klis, J. E. McClintock, M. R. Garcia, P. Zhao, R. K. Jain, C. D. Bailyn, and R. A. Remillard (2002, April). Dynamical Evidence for a Black Hole in the Microquasar XTE J1550-564. *ApJ 568*, 845–861.

Shabad, G. (2000). *Detection of High-Frequency Variability in a Black Hole Transient With USA*. Ph. D. thesis, Stanford Universtiy.

Suniaev, R. A. and J. Truemper (1979, June). Hard X-ray spectrum of CYG X-1. *Nature 279*, 506–508.

Sunyaev, R. and M. Revnivtsev (2000, June). Fourier power spectra at high frequencies: a way to distinguish a neutron star from a black hole. *AAP 358*, 617–623.

Tanaka, Y. and W. H. G. Lewin (1995). Black-hole binaries. In *X-ray Binaries*. Cambridge University Press.

Tanaka, Y. and N. Shibazaki (1996). X-ray Novae. *ARAA 34*, 607–644.

Tananbaum, H., H. Gursky, E. Kellogg, R. Giacconi, and C. Jones (1972, October). Observation of a Correlated X-Ray Transition in Cygnus X-1. *ApJL 177*, L5.

Uemura, M. and The Vsnet Collaboration Team (2002, January). Optical observations of XTE J1118+480 during the 2000 outburst. In *ASP Conf. Ser. 261: The Physics of Cataclysmic Variables and Related Objects*, pp. 561.

Vilhu, O. (2002, June). Mass transfer from the donor of GRS 1915+105. *AAP 388*, 936–939.